

The Thermal Structure of the Jovian Atmosphere¹

JOSEPH S. HOGAN, S. I. RASOOL AND THÉRÈSE ENCRENAZ

Institute for Space Studies, Goddard Space Flight Center, NASA, New York, N. Y.

(Manuscript received 9 May 1969, in revised form 17 July 1969)

ABSTRACT

Thermal structure calculations have been carried out for the atmosphere of Jupiter above the level of the dense clouds, for boundary conditions suggested by recent observations. The resulting models are characterized by an extensive region of dynamical control above the cloud level, and a thermal inversion in the mesosphere, produced by absorption of solar IR energy in the 3020 cm^{-1} band of methane. The infrared and microwave spectra corresponding to the computed thermal models are found to be in generally good agreement with observed infrared and microwave brightness temperatures of Jupiter. The effective temperatures of all of the thermal models are higher than the solar equilibrium value, and, thus, an internal heat source on Jupiter is suggested.

1. Introduction

During the past year, important new observations of Jupiter have provided the motivation for a re-investigation of the thermal structure of the Jovian atmosphere. First, several authors have recently re-evaluated the abundances of hydrogen, methane and ammonia in the atmosphere of Jupiter, by estimating the total amounts of these constituents above various temperature and pressure levels (Owen and Mason, 1968; Belton, 1969). It now appears that the atmospheric composition on Jupiter is similar to that of the sun, and that the hydrogen-helium ratio by volume may be as large as 5.0. Second, the brightness temperature of Jupiter has recently been measured at a number of IR wavelengths between 2 and $20\text{ }\mu$ by Gillett *et al.* (1969). Important suggestions of those observations are 1) that the brightness temperature of Jupiter in the atmospheric window near $5\text{ }\mu$ may be as high as 230 K , and may be characteristic of the temperature at the top of a thick cloud, and 2) that a temperature inversion may be present in the middle atmosphere. Finally, microwave measurements of Jupiter have been carried out at several wavelengths in the vicinity of the strong absorption by the numerous inversion lines of NH_3 in the $1\text{--}2\text{ cm}$ region (Law and Staelin, 1968; Welch, 1969). These measurements in the center and wings of the NH_3 inversion band provide further information on the atmospheric temperature distribution.

These new sets of data constitute separate constraints which must be satisfied by any acceptable model of the vertical structure of the Jovian atmosphere. A theoretical model should be consistent with the latest estimates of atmospheric composition, while leading to a

spectral distribution of radiative loss to space in agreement with the observed IR and microwave brightness temperatures.

We wish to report here on a calculation of temperature and density profiles for the atmosphere of Jupiter above the level of the dense clouds. Thermal structure calculations have been made for various combinations of temperature, total pressure and composition at this level. For each thermal model, the energy flux radiated by the planet at various IR and microwave wavelengths was also computed and compared with observations.

2. Vertical structure

In the present study, a steady-state distribution of temperature and density for the atmosphere of Jupiter above the cloud level is computed as follows. Basic atmospheric properties at the cloud level, including the cloud-top temperature, the mixing ratios of the major constituents (H_2 , He, CH_4 , NH_3) and the total pressure are adopted, and a zero-order vertical temperature profile above the clouds is specified. A consistent distribution of pressure and density is then determined, assuming the atmosphere to be in hydrostatic equilibrium. The concentrations of H_2 , He and CH_4 are computed with the assumption of a mixed atmosphere, and the mixing ratio of NH_3 is assumed to be constant at levels where NH_3 is unsaturated. At levels where NH_3 saturation occurs, the concentration of NH_3 is computed from a saturation formula derived from Lasker (1963), i.e.,

$$n_{\text{NH}_3}(T) = \frac{n_{\text{NH}_3}(145.0) \left(\frac{145.0}{T} \right)}{\exp \left[25.88 \left(\frac{145.0}{T} - 1.0 \right) \right]}$$

¹ This paper is a revised version of the remarks presented at the Conference, incorporating important suggestions made by Drs. R. Goody and M. B. McElroy in the Conference discussion.

where T is the temperature and $n_{\text{NH}_3}(145.0)$ the saturation number density of NH_3 at 145.0K, taken here to be $2.84 \times 10^{15} \text{ cm}^{-3}$.

For the zero-order structure obtained in this manner, the mean IR transmission of the atmosphere in wavelength intervals of interest is evaluated for required paths, considering contributions to the infrared opacity by pressure-induced absorption of H_2 and the vibration-rotation bands of CH_4 and NH_3 . Using these transmissions, the energies of planetary (7–100 μ) and solar (2–4 μ) origin absorbed per unit volume at various levels in the atmosphere are computed, and the total energy absorbed is equated to the 7–100 μ volumetric emission. The energy balance relationship is thus

$$\int \int [I(\nu, \theta, z) + S(\nu, \theta, z)] \sum_i n_i(z) k_i(\nu, z) d\nu d\omega \\ = \int \int J(\nu, z) \sum_i n_i(z) k_i(\nu, z) d\nu d\omega,$$

where $I(\nu, \theta, z)$ is the intensity of planetary radiation, $S(\nu, \theta, z)$ the solar intensity, $J(\nu, z)$ the atmospheric source function, $n_i(z)$ and $k_i(\nu, z)$ the number density and absorption coefficient of the i th constituent, and ν, θ, z and ω have their usual meanings.

In the above expression, $I(\nu, \theta, z)$ and $S(\nu, \theta, z)$ are evaluated by standard radiative transfer techniques. It is assumed that the cloud top radiates like a black-body in the 7–100 μ range, and that the downward directed intensity of planetary radiation at the upper boundary is negligible. $S(\nu, \theta, z)$ is computed for daily mean conditions at latitude 45°, equinox.

By relating the 7–100 μ emission (represented by the right-hand side of the above equation) to the temperature, assuming that local thermodynamic equilibrium conditions prevail at all levels under consideration, a first-order profile of temperature is obtained. The atmospheric structure is then recomputed for the first-order temperature distribution. Iteration of this procedure is performed until temperature convergence to within an arbitrarily small limit is achieved.

In the course of these calculations, whenever a super-adiabatic temperature gradient is obtained, the calculated lapse rate is replaced by the dry adiabatic lapse rate. In this manner, allowances are made for adjustments of unstable radiative profiles by dynamical processes in the optically thick region of the Jovian atmosphere adjacent to the clouds.

The release of latent heat in the NH_3 sublimation process would not significantly alter the basic thermal structure of the atmosphere, and this effect was not taken into account in the energy balance relationship.

In the present solution of the equation of radiative transfer, the IR regions between 2 and 4 μ and between 7 and 100 μ were divided, respectively, into 16 and 50 wavelength intervals of varying width. Higher resolution was adopted in regions where rapid variations of

absorption coefficient with wavelength occur, to obtain an acceptable simulation of the contours of absorption both in the CH_4 and NH_3 vibration-rotation bands and in the H_2 continuum.

Mean absorption coefficients for CH_4 in the 3020 and 1306 cm^{-1} bands were estimated from the measurements of Burch and Williams (1962), while absorption coefficients in the 3300, 1628 and 950 cm^{-1} bands of NH_3 were estimated from the measurements of France and Williams (1966). In extrapolating the CH_4 and NH_3 absorption coefficients to obtain their values under atmospheric conditions, the strong line approximation (Plass, 1960) was employed.

Coefficients for H_2 absorption, induced under high pressures by $\text{H}_2\text{-H}_2$ and $\text{H}_2\text{-He}$ collisions, were taken from Trafton (1967). Trafton's values were extrapolated to atmospheric conditions taking into account the strong pressure dependence (pressure²) of absorption of this type.

Values of the solar radiation in the 2–4 μ region incident on the top of the earth's atmosphere were obtained from the *Handbook of Geophysics* (Gast, 1960). In correcting these values for the orbital distance of Jupiter, the mean orbital radius of 5.203 A.U. was adopted.

Five thermal models of the Jovian atmosphere were constructed by the method outlined above, for cloud-top temperatures ranging from 210 to 230K, and for total pressures at the cloud level between 2.4 and 7.2 atm. The above range of temperature at the cloud top is consistent with the findings of Gillett *et al.* (1969), and also with the results of Owen (1965) and Danielson (1966), who deduced temperatures of $200 \pm 25\text{K}$ and $210 \pm 15\text{K}$, respectively, in the vicinity of the cloud top. The proportions by volume of H_2 , He, CH_4 and NH_3 were assumed to be 5.0:1.0:0.005:0.001. Basic characteristics of these model atmospheres are listed in Table 1, and the temperature profiles obtained in these cases are shown in Fig. 1.

In all five of the resulting thermal structures, a rather extensive region of dynamical control develops above the cloud level, with an adiabatic decrease in temperature from the cloud top to a "tropopause" in the 30–40 km altitude range. Above the "tropopause", temperatures continue to fall sub-adiabatically, to a low value near the 65-km level, but in all cases except Model 1, an increase in temperature with altitude is found at

TABLE 1. Model characteristics. ($\text{H}_2\text{:He:CH}_4\text{:NH}_3$ = 5.0:1.0:0.005:0.001).

Model no.	H_2 pressure at cloud top (atm)	Cloud-top temperature (°K)
1	2.0	220
2	4.0	230
3	4.0	220
4	4.0	210
5	6.0	220

levels above 65 km, as a result of near infrared solar heating in the 3020 cm^{-1} CH_4 band. As one might anticipate, the strength of this inversion is found to depend directly on the cloud-top pressure (opacity) for a given cloud-top temperature, and inversely on the cloud-top temperature for a given cloud-top pressure (opacity). No inversion appears in Model 1, but, rather, a general warming of the atmosphere at levels above the "tropopause" is found, as a consequence of the relatively low pressure, small far-infrared opacities, and warm radiative equilibrium temperatures which characterize this model.

Gillett *et al.* (1969) interpreted their IR observations of Jupiter as indicating the presence of an inversion in the Jovian atmosphere, and were the first to suggest that solar heating in the 3020 cm^{-1} CH_4 band could be responsible for its formation. Thus, the present calculations confirm their hypothesis. Solar UV photoionization and photodissociation energy is deposited well above the 100-km level in all of the models considered here, and does not affect the thermal structure of the atmosphere in the altitude range of interest.

The vertical distributions of H_2 , He, CH_4 and NH_3 corresponding to a typical model (Model 3) are shown in Fig. 2. Due to their extreme similarity to the pattern of Fig. 2, the density distributions for the other thermal models have been omitted. The sharp decrease in the NH_3 concentration between 30 and 45 km altitude is

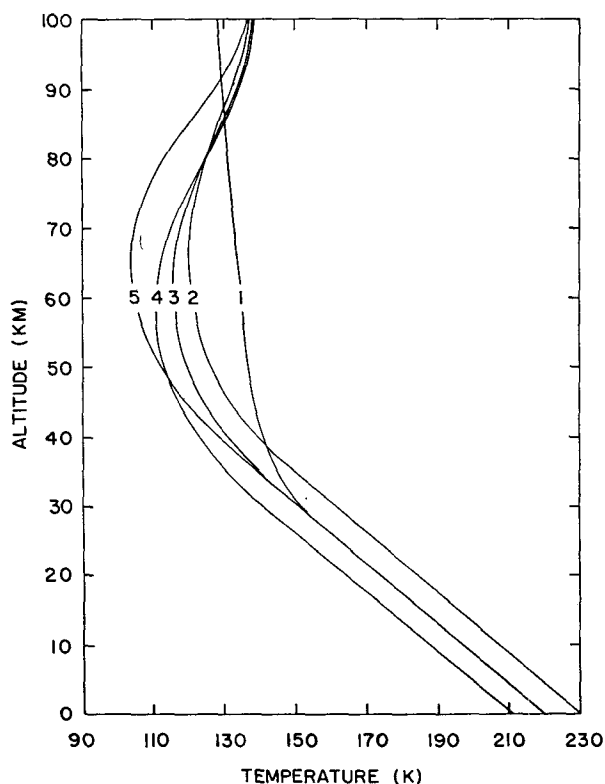


FIG. 1. Thermal models for the Jovian atmosphere.

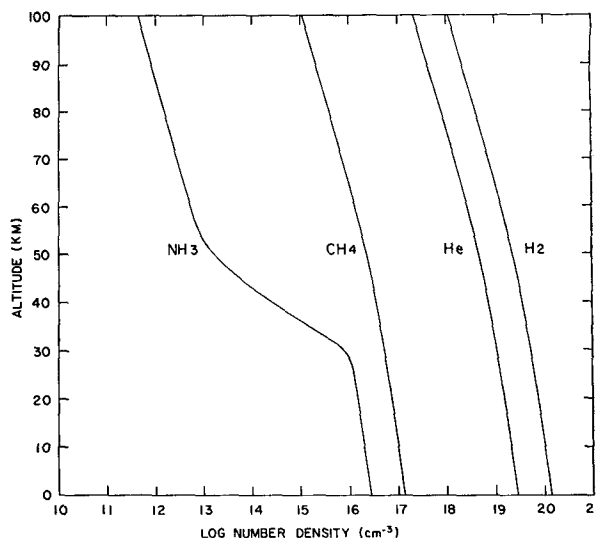


FIG. 2. Density distributions for H_2 , He, CH_4 and NH_3 , corresponding to thermal Model 3.

produced by NH_3 saturation near the 145K level. The maximum amount of NH_3 which could be deposited in this region is 0.65 gm cm^{-2} , the difference between the amount which would be present above the level of saturation if the sublimation process did not occur, and the amount present on the basis of a saturated NH_3 distribution. Even if all of this crystallized NH_3 were distributed uniformly over a 15-km altitude range, the corresponding density of solid material would be only $4.0 \times 10^{-7}\text{ gm cm}^{-3}$, of approximately the same magnitude as the density of cirrus clouds in the earth's atmosphere.

Similar estimates of the density of a thin cloud of solid NH_3 on Jupiter have been obtained by Lewis (1969). It appears unlikely that the presence of such clouds would modulate the transfer of far infrared radiation to any large extent. Indeed, the high brightness temperature observed near 5μ by Gillett *et al.* implies that the transmittance of these clouds is quite high at this wavelength. It is not unreasonable, therefore, to assume that they are equally transparent at longer wavelengths.

In Table 2, the total amounts of H_2 , He, CH_4 and NH_3 present above various temperature levels in the atmosphere of Model 3 are listed. These abundances agree in general with the estimates of Savage and

TABLE 2. Amounts of atmospheric constituents above various temperature levels for Model 3.

T (°K)	H_2 (km atm)	He (km atm)	CH_4 (m atm)	NH_3 (m atm)
220	150	20	150	21
200	114	23	114	14
180	80	16	80	7.6
160	55	11	55	2.6
140	36	7.2	36	0.15

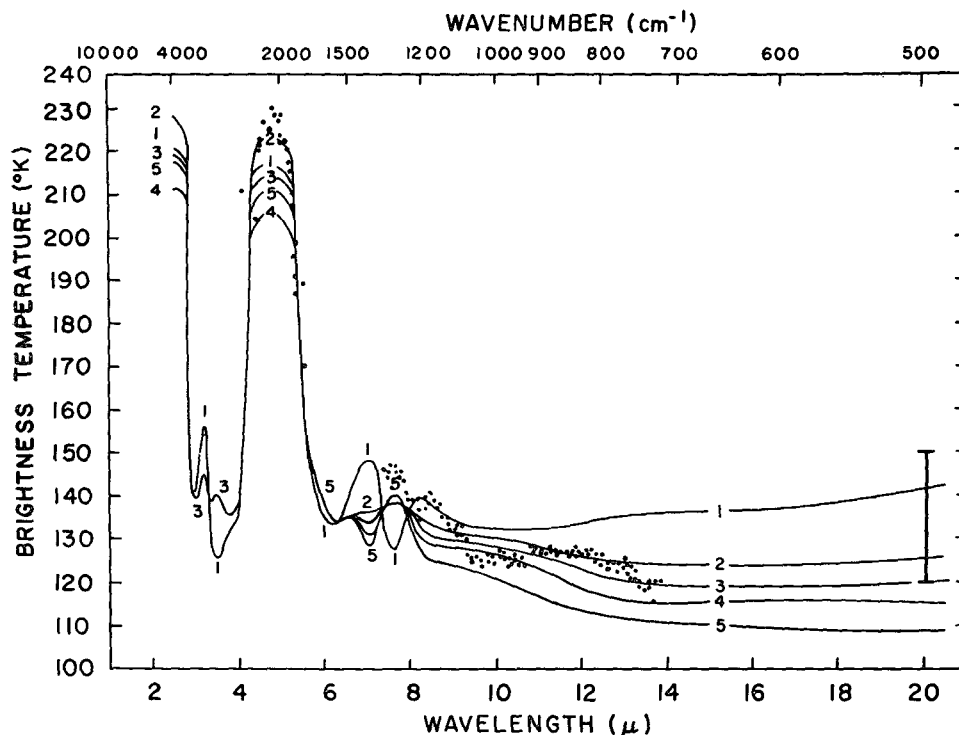


FIG. 3. Computed and observed infrared brightness temperatures of Jupiter. The dots correspond to the measurements of Gillett *et al.* (1969), while the vertical bar at 20μ wavelength corresponds to the range observed by Low (*loc. cit.*).

Danielson (1968), Owen and Mason (1968) and Belton (1969).

The effective temperature of the radiative losses to space corresponding to thermal Models 1–5 are 145K, 132K, 127K, 121K and 112K, respectively. A value of 140K for the effective temperature of Jupiter was measured by Low². Although the effective temperatures of the present models are generally somewhat lower than that observed by Low, they are, nevertheless, higher than the range of 88–105K, the solar equilibrium effective temperature corresponding to the range in the measured albedo of Jupiter of 0.73 (Harris, 1961) to 0.45 (Taylor, 1965). Our models, therefore, imply the existence of an internal heat source on Jupiter.

Atmospheric dynamics were taken into account in the present study only insofar as they might adjust the radiative structure of the atmosphere in unstable regions, via convection. No rigorous treatment of Jovian dynamics was included in the one-dimensional, steady-state problem considered here. However, the fact that an extensive convective zone develops in all of the present models, allows certain conclusions to be drawn about the importance of radiative transfer in determining the structure of the dense regions of the Jovian atmosphere adjacent to the clouds. From these calculations, it is clear that radiative transfer, acting alone, would produce a deep region characterized by a superadiabatic

temperature gradient. It is thus indicated that radiative coupling of atmospheric layers must be weak for a considerable distance above the cloud level. It is likely, therefore, that dynamical processes of one type or another would strongly influence the thermal structure in this region.

From their analysis of the relative magnitudes of the time constants for radiative and dynamical processes, Gierasch and Goody (1969) also concluded that the structure of the Jovian atmosphere is determined mainly by dynamics over an extensive altitude range. Their findings, which are based upon a more thorough analysis and direct approach to the problem, are supported by the results of the present study.

Regardless of the nature of the dynamical processes which determine the structure of the atmosphere above the cloud level, the end result must be the production of a zone of adiabatic temperature gradient, similar to the "troposphere" which develops in the present models. The thickness of the "troposphere" would depend upon the strength of the circulation responsible for its formation, but could be no less than the thickness computed here, on the basis of a convective adjustment of the radiative temperature profile. On the other hand, were this zone of dynamical influence to extend to much higher altitudes, the atmospheric inversion would be suppressed by dynamical redistribution of the thermal energy. In that case, no atmospheric inversion would be in evidence in the IR spectrum of Jupiter. Therefore,

² Paper presented at Third Arizona Conference on Planetary Atmospheres.

it appears unlikely that dynamical processes would greatly modify the structure of the Jovian atmosphere from the basic pattern of Fig. 1.

3. Infrared brightness temperature

For each of the five thermal models of the Jovian atmosphere, the radiative flux emanating from the planet at various IR wavelengths was calculated from radiative transfer theory, and a brightness temperature at each wavelength was derived. In the determination of brightness temperature, the transmission of the atmosphere at wavelengths of interest was obtained in the manner previously described.

In Fig. 3, the resulting IR brightness temperatures for the five thermal models are shown. The basic patterns which emerge are similar in all five cases, and in those spectral regions where near overlapping of several brightness temperature curves occurs, some of the curves have been omitted to avoid confusion.

The low value of brightness temperature found between 3 and 4 μ is a result of strong absorption in the 3020 cm^{-1} CH_4 band, while the smaller feature at 3 μ is due to the 3300 cm^{-1} band of NH_3 . The 1628 cm^{-1} NH_3 band produces the low brightness temperatures near 6 μ , while the 1306 cm^{-1} CH_4 band provides the opacity in the 7–8.5 μ region. Atmospheric absorption between 8.5 and 12 μ is mainly due to the broad 950 cm^{-1} band of NH_3 but includes a component due to H_2 which increases with wavelength in this range. At wavelengths $>12 \mu$, the NH_3 opacity decreases rapidly, and H_2 absorption is primarily responsible for the computed brightness temperatures beyond 12 μ . The H_2 opacity reaches a maximum near 17 μ , and decreases again at longer wavelengths.

The effect of the atmospheric inversion on the calculated brightness temperatures can be discerned in three spectral regions where strong absorption is present, i.e., near the centers of the 3020 cm^{-1} CH_4 band, the 1628 cm^{-1} NH_3 band, and the 1306 cm^{-1} CH_4 band.

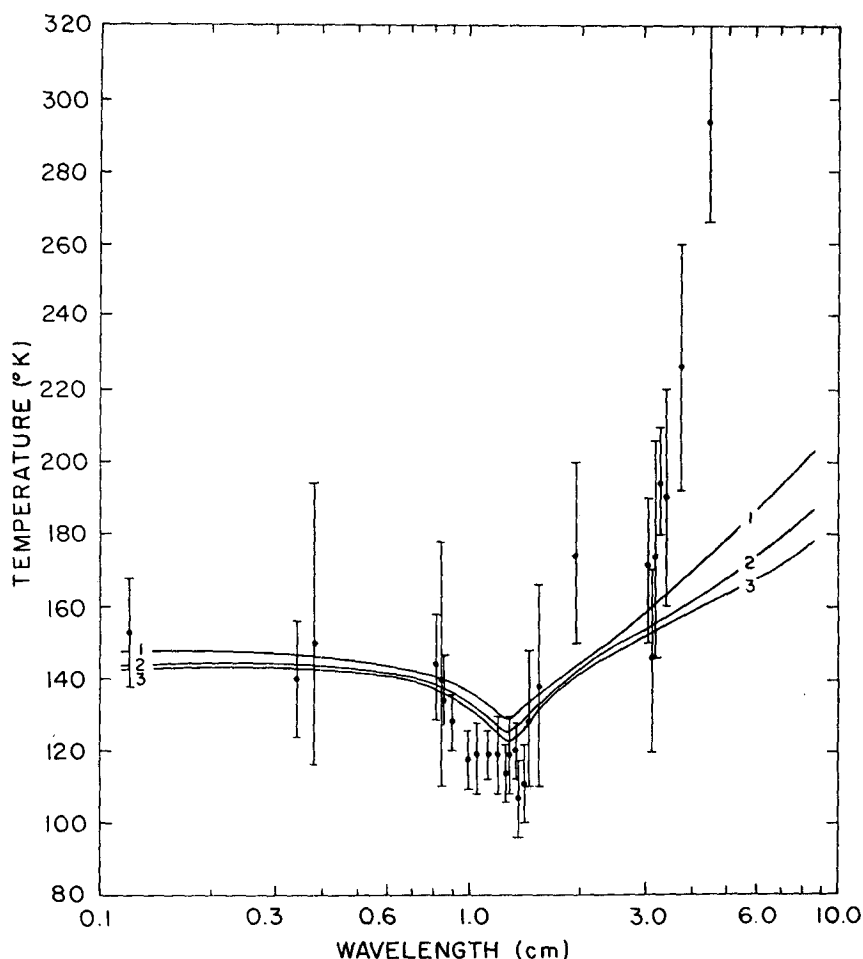


FIG. 4. Computed and observed microwave brightness temperatures of Jupiter. The computed values (indicated by solid curves) include only the thermal component, while the observed brightness temperatures (indicated by vertical bars) include a nonthermal component which becomes quite large at wavelengths $>3 \text{ cm}$.

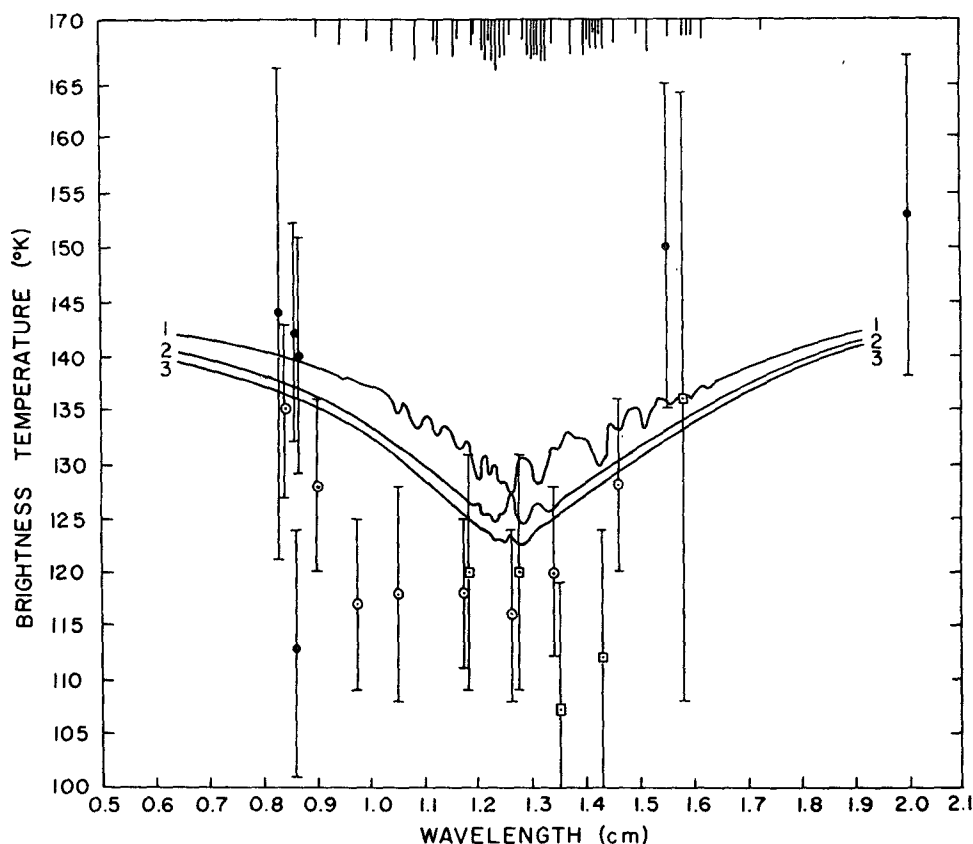


FIG. 5. Computed and observed microwave brightness temperatures of Jupiter near the center of the NH_3 inversion band. Vertical lines at the top of the figure indicate the position of the strongest lines in this region.

In the strong regions of these bands, the highest brightness temperatures are found in the most opaque models. In Model 1, a "low opacity" model where no inversion is present, local minima in brightness temperature are computed at 3.3 and 7.7μ near the centers of the CH_4 bands. However, in Model 3, for example, a model of medium opacity where an inversion develops, local maxima are found at these wavelengths.

Also plotted in Fig. 3 are points corresponding to the measurements of Gillett *et al.* (1969) and Low (*loc. cit.*). Earlier observations of brightness temperature in the $8\text{--}14 \mu$ range have resulted in values between 120 and 140K (Menzel *et al.*, 1926; Sinton and Strong, 1960; Murray and Wildey, 1963; Sinton, 1964). As can be seen, the calculated values are in general accord with the observations in the $7\text{--}14 \mu$ range, with a tendency toward the observed elevation in brightness temperature between 7 and 9μ due to the atmospheric inversion in Models 2–5. Good agreement with the measured brightness temperatures in the atmospheric "window" between 4 and 5μ is also obtained. Best overall agreement with the observations is found in the case of Model 3.

As mentioned earlier, in all of the models presented here, the same atmospheric composition was adopted ($\text{H}_2:\text{He}:\text{CH}_4:\text{NH}_3 = 5.0:1.0:0.005:0.001$). Agreement

with the observations of Gillett *et al.* could undoubtedly be improved by adjusting the relative concentrations of these constituents. For example, a change in the concentration of NH_3 at higher levels in the models, perhaps due to the use of an alternate NH_3 saturation relationship, would modify the calculated pattern of brightness temperature in the $8.5\text{--}12 \mu$ wavelength region, with little influence on the pattern outside of this range. Through such adjustments it might be possible to obtain more refined estimates of atmospheric composition. However, no attempt to derive such refined estimates was made in the present study, in view of the inherent lack of precision involved in the determination of the transmission characteristics of the atmosphere in the present manner.

It appears from these calculations, that the atmospheric inversion observed by Gillett *et al.* in the 1306 cm^{-1} CH_4 band should also be detectable from high-resolution measurements across the 3020 cm^{-1} band of CH_4 .

4. Microwave spectrum of Jupiter

The brightness temperature of Jupiter at microwave wavelengths ($0.1\text{--}10.0 \text{ cm}$) was also computed for each

thermal structure model. Strong atmospheric absorption occurs on Jupiter between 11,900 and 40,000 MHz in the microwave region due to the NH_3 inversion effect. In these calculations, the 92 NH_3 inversion lines which have been observed (Townes and Schawlow, 1955; Nishikawa and Shimoda, 1955) have been taken into account.

At each frequency of interest, the molecular absorption coefficient due to each line was computed following Townes and Schawlow, assuming the Van Vleck-Weisskopf line shape. The half-width was assumed to be due to foreign broadening of NH_3 by H_2 and He. According to Anderson (1950), the most important interaction in this case is between the quadrupolar momentum of NH_3 and the induced dipolar momentum of H_2 and He, and the cross section for this interaction has been computed following his development. By summing the contributions from each NH_3 line, as well as the contribution from pressure-induced H_2 absorption, the total opacity at each frequency was obtained.

With a knowledge of the total absorption coefficient at each point in the atmosphere, the brightness temperature was determined by standard radiative transfer techniques. The results for thermal Models 1, 2 and 3 are shown in Figs. 4 and 5, where a comparison with observations [tabulated by Law and Staelin (1968) and Goodman (1969)] is made; also included are the recent observations of Welch (1969). As can be seen from Fig. 4, general agreement with the observations is obtained at wavelengths < 3 cm in the 0.1–10.0 cm range. The minimum in brightness temperature observed between 1 and 2 cm in the region of strong NH_3 absorption is well replicated in the three cases shown. At wavelengths > 3 cm, divergence between observed and computed brightness temperatures is found due to a nonthermal component in the observations which increases as the square of the wavelength. The computed thermal component increases with wavelength in a similar fashion due to the asymmetric form of the assumed line shape. The Van Vleck-Weisskopf profile produces a slowly varying absorption coefficient at wavelengths distant from the line center on the short-wavelength wing, while on the long-wavelength wing the absorption coefficient varies inversely as the square of the wavelength.

As wavelength increases, the thermal component of brightness temperature computed here converges asymptotically to a value characteristic of the lower boundary temperature of the model, since sources of radiation below the top of the dense cloud layer were not considered. Therefore, in the present study, the thermal brightness temperatures near 10 cm wavelength have been underestimated. In fact, an observational value of $260 \pm 26\text{K}$ was deduced for the thermal component at 10.4 cm wavelength by Berge (1966).

A more detailed depiction of brightness temperatures in the region of strong absorption is shown in Fig. 5 for Models 1, 2 and 3. Although the minimum temperatures computed at the center of the NH_3 band agree

well with the observations, the computed temperatures are warmer than those observed in the 0.95–1.05 cm and 1.35–1.45 cm ranges by some 10K. The reasons for this discrepancy are unclear.

The most interesting aspect of this figure is the evidence of the atmospheric inversion which appears in the brightness temperature curves of Models 2 and 3. In Model 1, where no inversion is present, the lowest brightness temperatures are found at wavelengths where strongest absorption occurs. In Models 2 and 3, however, the atmospheric inversion produces elevated temperatures (by as much as 5K) at these wavelengths. These models are consistent with the findings of Wrixon³ who reports evidence of a thermal inversion in recent microwave observations of Jupiter.

5. Conclusions

These calculations indicate that thermal models of atmospheric structure, computed for boundary conditions suggested by recent observations of Jupiter, give rise to IR and microwave spectra which are in good agreement with measurements of the Jovian brightness temperatures in these spectral regions. Although the present method of evaluating atmospheric transmissions in the IR region is probably not precise enough to permit a meaningful refinement of atmospheric composition estimates, it is felt that the models derived here are fundamentally sound, and sufficiently accurate to reveal several basic features of the Jovian atmosphere:

- 1) There is an extensive "troposphere" overlying the dense clouds on Jupiter, in which the atmospheric structure is determined by dynamical processes.
- 2) A thermal inversion of about 30K, produced by solar IR heating in the 3020 cm^{-1} CH_4 band, is present in the mesosphere, as suggested by Gillett *et al.* on the basis of their observations.
- 3) The effective temperature of the atmosphere is significantly higher than that computed on the basis of solar equilibrium. A model with a temperature and pressure at the cloud level of 220K and 4.8 atm, respectively, while producing the best overall agreement with the observed IR brightness temperatures, is characterized by a radiative loss to space which is approximately twice that required to balance the interacting solar flux for an albedo of 0.45. An internal source of energy on Jupiter is therefore implied.

Acknowledgements. The authors wish to thank Dr. R. W. Stewart for his helpful advice and criticism. One of the authors (J. S. H.) was supported by a National Academy of Sciences—National Research Council Associateship, while another (T. E.) held a European Space Research Organization Fellowship at the Goddard Institute for Space Studies.

Note added in proof. Recently, alternate models of

³ Paper presented at Third Arizona Conference on Planetary Atmospheres.

the Jovian atmosphere were constructed for H_2 -He ratios as small as 1.0:1.0. One effect of a decrease in this ratio is the production of a colder atmosphere in the vicinity of the cloud level due to the larger adiabatic gradient associated with the increased proportion of He. However, increasing the He concentration also produces an overall decrease in the IR opacity of the atmosphere, so that the "troposphere" becomes less extensive while the mesosphere becomes generally warmer. As a further consequence, the atmospheric inversion becomes considerably less pronounced.

It is found that the best overall agreement with the IR and microwave spectra of Jupiter is obtained for a 5.0:1.0 H_2 -He ratio. Discrepancies between calculated and observed brightness temperatures become larger as the concentration of He is increased. The present results indicate, therefore, that a large value (5.0:1.0) for the H_2 -He ratio on Jupiter is most consistent with the observed Jovian brightness temperatures.

REFERENCES

- Anderson, P. W., 1950: Pressure broadening of the ammonia inversion line by foreign gases: Quadrupole-induced dipole interactions. *Phys. Rev.*, **80**, 511-513.
- Belton, M. J. S., 1969: An estimate of the abundance and the rotational temperature of CH_4 on Jupiter. *Astrophys. J.*, **157**, 469-472.
- Berge, G. L., 1966: An interferometric study of Jupiter's decimeter radio emission. *Astrophys. J.*, **146**, 767-798.
- Burch, D. E., and D. Williams, 1962: Absorption by nitrous oxide, carbon monoxide and methane. Infrared absorption by carbon dioxide, water vapor and minor atmospheric constituents, Part B. Rept. AFCRL-62-698, Air Force Cambridge Research Laboratories.
- Danielson, R. E., 1966: The infrared spectrum of Jupiter. *Astrophys. J.*, **143**, 949-960.
- France, W. L., and D. Williams, 1966: Total absorptance of ammonia in the infrared. *J. Opt. Soc. Amer.*, **56**, 70-74.
- Gast, P. R., 1960: Solar radiation. *Handbook of Geophysics*, Air Force Cambridge Research Center, New York, MacMillan, 16-14 to 16-32.
- Gierasch, P., and R. Goody, 1969: Radiative time constants in the atmosphere of Jupiter. *J. Atmos. Sci.*, **26**, 979-980.
- Gillett, F. C., F. J. Low and W. A. Stein, 1969: The 2.8-14 μ spectrum of Jupiter. *Astrophys. J.*, **157**, 925-934.
- Goodman, G. C., 1969: Models of Jupiter's atmosphere. Ph.D. thesis, University of Illinois.
- Harris, D. L., 1961: Photometry and colorimetry of planets and satellites. *Planets and Satellites, The Solar System*, Vol. 3, University of Chicago Press, 272-342.
- Lasker, B. M., 1963: Wet adiabatic model atmospheres for Jupiter. *Astrophys. J.*, **138**, 709-719.
- Law, S. E., and D. H. Staelin, 1968: Measurements of Venus and Jupiter near 1 cm wavelength. *Astrophys. J.*, **154**, 1077-1086.
- Lewis, J. S., 1969: The clouds of Jupiter and the NH_3 - H_2O and NH_3 - H_2S systems. *Icarus* (in press).
- Menzel, D. H., W. W. Coblentz and C. O. Lampland, 1926: Planetary temperatures derived from water-cell transmissions. *Astrophys. J.*, **63**, 177-187.
- Murray, B. C., and R. L. Wildey, 1963: Stellar and planetary observations at 10 microns. *Astrophys. J.*, **137**, 692-693.
- Nishikawa, T., and K. Shimoda, 1955: Inversion spectrum of ammonia. *J. Phys. Soc. Japan*, **10**, 89-92.
- Owen, T., 1965: Comparisons of laboratory and planetary spectra. II. The spectrum of Jupiter from 9700 to 11200 \AA . *Astrophys. J.*, **141**, 444-456.
- , and H. P. Mason, 1968: The abundance of hydrogen in the atmosphere of Jupiter. *Astrophys. J.*, **154**, 317-326.
- Plass, G. N., 1960: Useful representations for measurements of spectral band absorption. *J. Opt. Soc. Amer.*, **50**, 868-875.
- Savage, B. D., and R. E. Danielson, 1968: Models of the atmosphere of Jupiter. *Infrared Astronomy*, New York, Gordon and Breach, 211-244.
- Sinton, W. M., 1964: Physical researches on the brighter planets. Rept. AFCRL-64-926, Air Force Cambridge Research Laboratories.
- , and J. Strong, 1960: Radiometric observations of Venus. *Astrophys. J.*, **131**, 470-490.
- Taylor, D. J., 1965: Spectrophotometry of Jupiter's 3400-10000 \AA spectrum and a bolometric albedo for Jupiter. *Icarus*, **4**, 362-373.
- Townes, C. H., and A. L. Schawlow, 1955: *Microwave Spectroscopy*. New York, McGraw-Hill, 698 pp.
- Trafton, L. M., 1967: Model atmospheres of the major planets. *Astrophys. J.*, **147**, 765-781.
- Welch, W. J., 1969: *Icarus* (in press).